Biophysical Chemistry, 44 (1992) 29–45
Elsevier Science Publishers B.V., Amsterdam

BIOCHE 01672

The vibrational normal modes of β-barrels in an IgG antibody molecule

Wen-Ge Han and Cun-da Wang
Department of Physics, Tianjin University, Tianjin 300072 (People's Republic of China)

(Received 2 January 1992; accepted 4 March 1992)

Abstract

Based on the quasi-continuity model, and using the method of group theory, we studied the normal vibrations of the V_L- and the C_{HL}-β-barrels in an IgG molecule. We put emphasis on the Raman- and the infrared-active normal modes. The Raman modes we obtained include both the breathing motion mode (or the dominant low-frequency mode) which corresponds to the maximum peak in the Raman spectrum, and the normal modes that correspond to the lower peaks. Our calculated vibration frequencies are found to be in good agreement with the experimental results observed by Painter et al. (Biopolymers 20 (1981) 243). The method and work presented in this paper may improve Chou's quasi-continuity theory in calculating the vibrational modes of a β-barrel protein.

Keywords: Immunoglobulin G antibody molecule; β-barrel; Quasi-continuity model; Group D_{7h} symmetry species; Raman and infrared active vibrational normal modes

1. Introduction

The low-frequency Raman modes with wave numbers ranging from 10–60 cm^{-1} have been observed in many kinds of biomacromolecules [1–5]. These internal vibrational modes are very sensitive to the conformational changes of the biomacromolecules, and indeed play a significant role in biological functions. In order ot reveal the physical mechanisms of such interesting internal motions, several models such as the elastic global model [6], the normal mode model [7–9] and the quasi-continuity model [11–17], have been proposed. Each model has its own criteria. They all contribute to the development of this research field. Chou summarized them in his review article [17].

Using the quasi-continuity model, Chou calculated the dominant low-frequency modes of some biomacromolecules [17]. These modes correspond to the maximum peaks in the Raman spectra of these molecules. However, one should notice that, in the Raman spectrum, there are still several small peaks beside the maximum one. Therefore, in addition to the dominant low-frequency mode, there also exist other vibrational modes in the biomacromolecules.

The low-frequency Raman spectrum of bovine antibody molecule immunoglobulin G (IgG) was

Correspondence to: Dr. W.-G. Han, Department of Physics, Tianjin University, Tianjin 300072 (People's Republic of China).

obtained by Painter et al. [3]. There are three conspicuous peaks at 28 cm^{-1}, 36 cm^{-1}, and 60 cm^{-1} in the spectrum.

In this paper, based on Chou's quasi-continuity model and using the method of group theory, we calculate the vibrational normal modes of some β-barrels in an IgG molecule. The vibrational frequencies we obtained are found to be in good agreement with Painter's experimental results.

2. The quasi-continuity model

The conformation of an IgG molecule is shown in Fig. 1. It consists of two identical heavy (H) and two identical light (L) polypeptide chains, which are folded to form 12 domains. As Chou described [16], each heavy chain contains four domains named V_H, C_H^1, C_H^2 and C_H^3, and each light chain contains two domains named V_L and C_L. An IgG molecule is made up of such 12 distinct domains, each of which contains a β-barrel. The β-barrel located in the V_H and V_L domains are termed the V_H-barrels and V_L-barrels, respectively. All the β-barrels located in the C_L, C_H^1, C_H^2 and C_H^3 domains are termed C_{HL}-barrels. There are two V_H-barrels, two V_L-barrels and eight C_{HL}-barrels in an IgG molecule. The number of strands is nine in a V_H-barrel and seven in a V_L- and a C_{HL}-barrel [16].

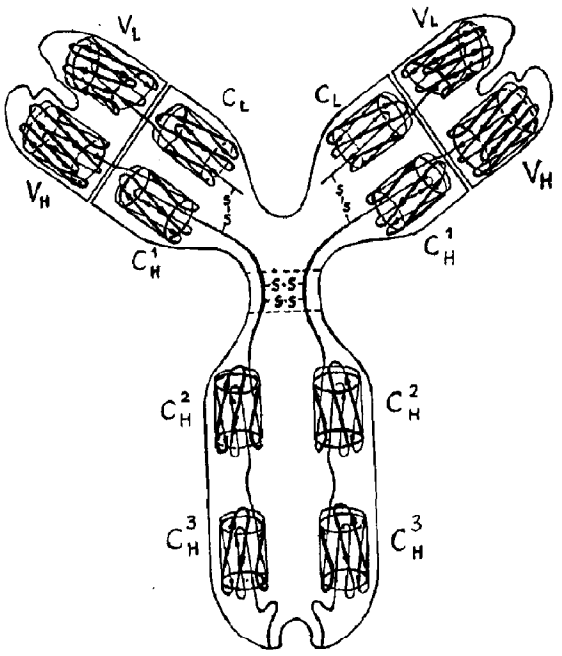

Fig. 1. Schematic drawing for an IgG molecule. (Reproduced from Fig. 1 of Ref. [16].)

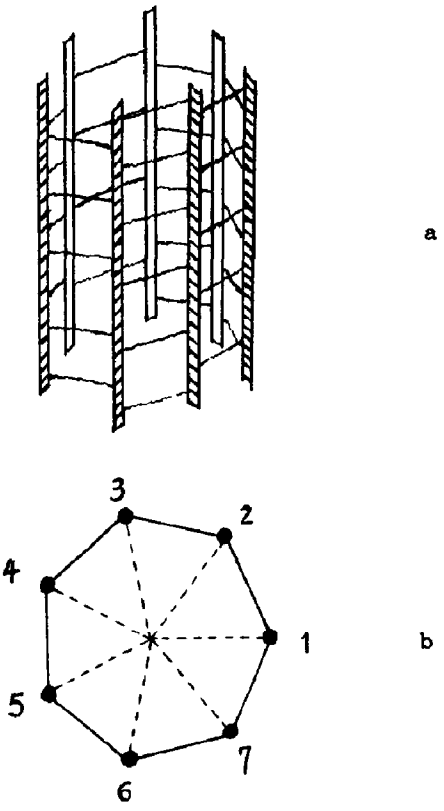

Fig. 2. (a) The "rods and springs" cylinder which represents a β-barrel with seven strands. (b) The normal section of such a cylinder which is a regular heptagon. (Adapted from Fig. 9 of Ref. [17].)

According to the quasi-continuity model, a β-barrel with seven strands can be considered as a "rods and springs" cylinder whose normal section is a regular heptagon (see Fig. 2). Each spring represents a hydrogen bond. The average number of springs between any two adjacent strands is λ. Each rod (or strand) represents a polypeptide chain. The mass m of each strand and the number λ vary with different kinds of seven-strand β-barrels.

From Fig. 1 we can see that the 10 V_L- and C_{HL}-barrels form the main part of an IgG molecule. Therefore, the Raman spectrum of an IgG molecule is mainly determined by the vibrational modes of its V_L- and C_{HL}-barrels which will be studied in this paper.

The strands in a V_L-barrel and in a C_{HL}-barrel are of the same number, seven. Both of these two kinds of β-barrels can be modeled as shown in Fig. 2. The symmetry of the regular heptagonal structure belongs to the group D_{7h}. We will use the method of group theory to find the Raman and the infrared active normal modes of such a structure in the following sections. Now let us review the characteristics of the group D_{7h}.

3. The group D_{7h}

In the model depicted in Fig. 2, there are 28 kinds of symmetrical operation which correspond to the 28 elements in the group D_{7h}. They are $\{E, C_7, C_7^2, C_7^3, C_7^4, C_7^5, C_7^6, 7C_2', \sigma_h, S_7, S_7^2, S_7^3, S_7^4, S_7^5, S_7^6, 7\sigma_v\}$. E is the identity operation. C_7^n ($n = 1, 2, \ldots 6$) means a rotation by $2\pi n/7$ about the sevenfold rotation z-axis (see Fig. 3). Each C_2' means a rotation by π about each twofold rotation axis C_2'. σ_h is the symbol for a reflection through the xy-plane. S_7^n ($n = 1, 2, \ldots 6$) refers to the operation in which n successive rotations of $2\pi/7$ about z-axis are carried out, each rotation being followed by a reflection in the xy-plane. Each σ_v represents a reflection through a σ_v-plane.

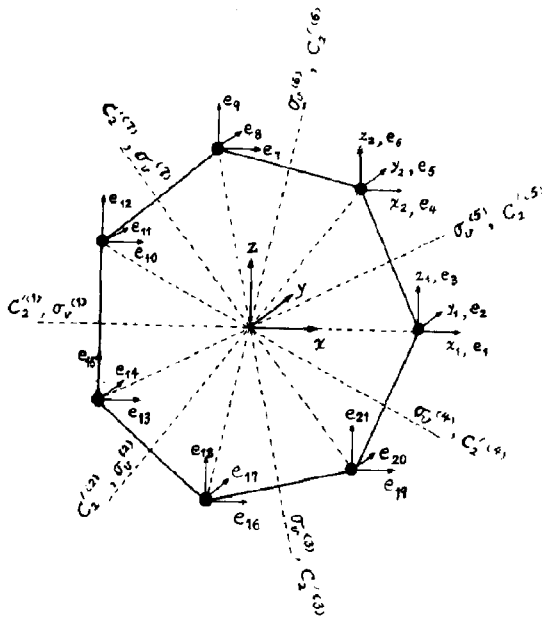

Fig. 3. Symmetry of the cylinder with seven strands.

Table 1

The characters of the irreducible representations A_1'–E_3'' of D_{7h}, and the characters of the representation $D(R)$ of D_{7h} formed by transformations of the displacement coordinates of our model

D_{7h}	E	C_7, C_7^6	C_7^2, C_7^5	C_7^3, C_7^4	$7C_2'$	σ_h	S_7, S_7^6	S_7^2, S_7^5	S_7^3, S_7^4	$7\sigma_v$	
A_1'	1	1	1	1	1	1	1	1	1	1	$(\alpha_{xx}+\alpha_{yy}, d_{zz})$
A_2'	1	1	1	1	−1	1	1	1	1	−1	R_z
A_1''	1	1	1	1	1	−1	−1	−1	−1	−1	
A_2''	1	1	1	1	−1	−1	−1	−1	−1	1	T_z
E_2'	2	$2\cos\frac{2\pi}{7}$	$2\cos\frac{4\pi}{7}$	$2\cos\frac{6\pi}{7}$	0	2	$2\cos\frac{2\pi}{7}$	$2\cos\frac{4\pi}{7}$	$2\cos\frac{6\pi}{7}$	0	(T_x, T_y)
E_1''	2	$2\cos\frac{2\pi}{7}$	$2\cos\frac{4\pi}{7}$	$2\cos\frac{6\pi}{7}$	0	−2	$-2\cos\frac{2\pi}{7}$	$-2\cos\frac{4\pi}{7}$	$-2\cos\frac{6\pi}{7}$	0	(R_x, R_y), $(\alpha_{xz}, \alpha_{yz})$
E_2'	2	$2\cos\frac{4\pi}{7}$	$2\cos\frac{6\pi}{7}$	$2\cos\frac{2\pi}{7}$	0	2	$2\cos\frac{6\pi}{7}$	$2\cos\frac{6\pi}{7}$	$2\cos\frac{2\pi}{7}$	0	$(\alpha_{xx}-\alpha_{yy}, \alpha_{xy})$
E_2''	2	$2\cos\frac{4\pi}{7}$	$2\cos\frac{6\pi}{7}$	$2\cos\frac{2\pi}{7}$	0	−2	$-2\cos\frac{4\pi}{7}$	$-2\cos\frac{6\pi}{7}$	$-2\cos\frac{2\pi}{7}$	0	
E_3'	2	$2\cos\frac{6\pi}{7}$	$2\cos\frac{2\pi}{7}$	$2\cos\frac{4\pi}{7}$	0	2	$2\cos\frac{6\pi}{7}$	$2\cos\frac{2\pi}{7}$	$2\cos\frac{4\pi}{7}$	0	
E_3''	2	$2\cos\frac{6\pi}{7}$	$2\cos\frac{2\pi}{7}$	$2\cos\frac{4\pi}{7}$	0	−2	$-2\cos\frac{2\pi}{7}$	$-2\cos\frac{2\pi}{7}$	$-2\cos\frac{4\pi}{7}$	0	
$D(R)$	21	0	0	0	−1	7	0	0	0	1	

The group D_{7h} is the direct product of group D_7 and C_s, that is $D_{7h} = D_7 \times C_s$. The group D_7 has 14 elements $\{E, C_7, C_7^2, C_7^3, C_7^4, C_7^5, C_7^6, 7C_2'\}$, and the group C_s has two elements $\{E, \sigma_h\}$. We can obtain the irreducible representation of group D_7 and C_s easily [18]. By combining each irreducible representation of D_7 with each of C_s, we can construct systematically all irreducible representations of group D_{7h}. The group D_{7h} has four one-dimensional and six two-dimensional irreducible representations. We list the characters of these representations in Table 1, where A_1', A_2', A_1'' and A_2'' are one-dimensional representations, and E_1', E_1'', E_2', E_2'', E_3' and E_3'' are two-dimensional ones. The last row of Table 1 lists the characters of a reducible representation $D(R)$ of D_{7h}. We will elaborate further on this in the next section.

In Table 1, we also indicate the symmetry species associated with translations, rotations and polarizability components. The symbols T_x, T_y and T_z represent the translations along the x-, y- and z-axis, respectively. R_x, R_y and R_z refer to the rotations about the x-, y- and z-axis, respectively. The polarizability components are represented as α_{xx}, α_{xy}, etc.

It is well known that the vibrational frequencies of the three translations and three rotations are zero. Therefore, a non-linear molecule with N atoms has $3N$-6 vibrational normal modes [18]. Our model of Fig. 2 should have $3 \times 7 - 6 = 15$ normal modes. Now let us study the symmetry species of these 15 kinds of normal modes and select the Raman and the infrared active ones.

4. The symmetry of the normal modes

The Cartesian coordinates of each rod are marked in Fig. 3. Let $e_1 = x_1$, $e_2 = y_1$, $e_3 = z_1$, $e_4 = x_2, \ldots, e_{21} = z_7$. Taking $\{e_1, e_2, \ldots, e_{21}\}$ as a basis, we can obtain a 21-dimensional representation $D(R)$ of group D_{7h} (R can represent any operation in D_{7h}). After reducing $D(R)$ into the direct sum of the irreducible representations, we can find out the number of vibrational normal coordinates with each symmetry.

By applying operation E to the basis $\{e_1, e_2, \ldots, e_{21}\}$, we have $Ee_1 = e_1$, $Ee_2 = e_2, \ldots, Ee_{21} = e_{21}$, therefore,

$$D(E) = \begin{bmatrix} 1 & & & \\ & 1 & & \\ & & \ddots & \\ & & & 1 \end{bmatrix}_{21\times 21}$$

and the character of $D(E)$ is $\chi_E = 21$.

Similarly, we can obtain all the other representational matrices such as $D(C_1)$, $D(\sigma_h)$, etc. We have listed the characters of the representation $D(R)$ on the last line of Table 1.

Now, we reduce the representation $D(R)$. Let $n^{(j)}$ be the number of times the jth irreducible representation of D_{7h} appears in the completely reduced form of $D(R)$. Then [18]

$$n^{(j)} = \frac{1}{g} \sum_R \chi_R^{(j)*} \chi_R, \tag{1}$$

where g is the number of operations in group D_{7h} (here $g = 28$) and the sum is over all these operations. $\chi_R^{(j)}$ is the character of the jth irreducible representation for the operation R, and the asterisk denotes the complex conjugate. χ_R is the character of $D(R)$ for the operation R. The values of $\chi_R^{(j)}$ and χ_R are listed in table 1.

As an example, the number of times $n^{(A_1')}$ of the irreducible representation A_1' appearing in the completely reduced form of $D(R)$ is

$$\begin{aligned} n^{(A_1')} &= \frac{1}{g} \sum_R \chi_R^{(A_1')*} \chi_R \\ &= \tfrac{1}{28}[1 \times 21 + 7 \times (-1) + 1 \times 7 + 7 \times 1] \\ &= 1. \end{aligned} \tag{2}$$

That means there is one normal coordinate with symmetry A_1'.

Similarly, we can obtain

$$\begin{aligned} &n^{(A_2')} = 1, \quad n^{(A_1'')} = 0, \quad n^{(A_2'')} = 1, \\ &n^{(E_1')} = 2, \quad n^{(E_1'')} = 1, \quad n^{(E_2')} = 2, \\ &n^{(E_2'')} = 1, \quad n^{(E_3')} = 2, \quad n^{(E_3'')} = 1. \end{aligned} \tag{3}$$

Therefore, the structure of the representation $D(R)$ is

$$\begin{aligned} D(R) = {} & A_1' + A_2' + A_2'' + 2E_1' + E_1'' \\ & + 2E_2' + E_2'' + 2E_3' + E_3''. \end{aligned} \tag{4}$$

These 21 coordinates include, of course the three coordinates representing translations and the three representing rotations. From Table 1, we can see that T_z belongs to the representation A_2'', and T_x, T_y to E_1', i.e.

$$D_{\text{trans}} = A_2'' + E_1'. \tag{5}$$

We also see that R_z to A_2', and R_x, R_y to E_1'', i.e.

$$D_{\text{rot}} = A_2' + E_1''. \tag{6}$$

Now by subtracting eqs. (5) and (6) from (4), we obtain finally

$$D_{\text{vib}} = A_1' + E_1' + 2E_2' + E_2'' + 2E_3' + E_3'', \tag{7}$$

which represents the 15 normal vibrations of our model in Fig. 2.

According to the selection rules for the Raman effect [18], only those normal vibrations which fall into the symmetry species associated with the polarizability components, will occur in the Ra-

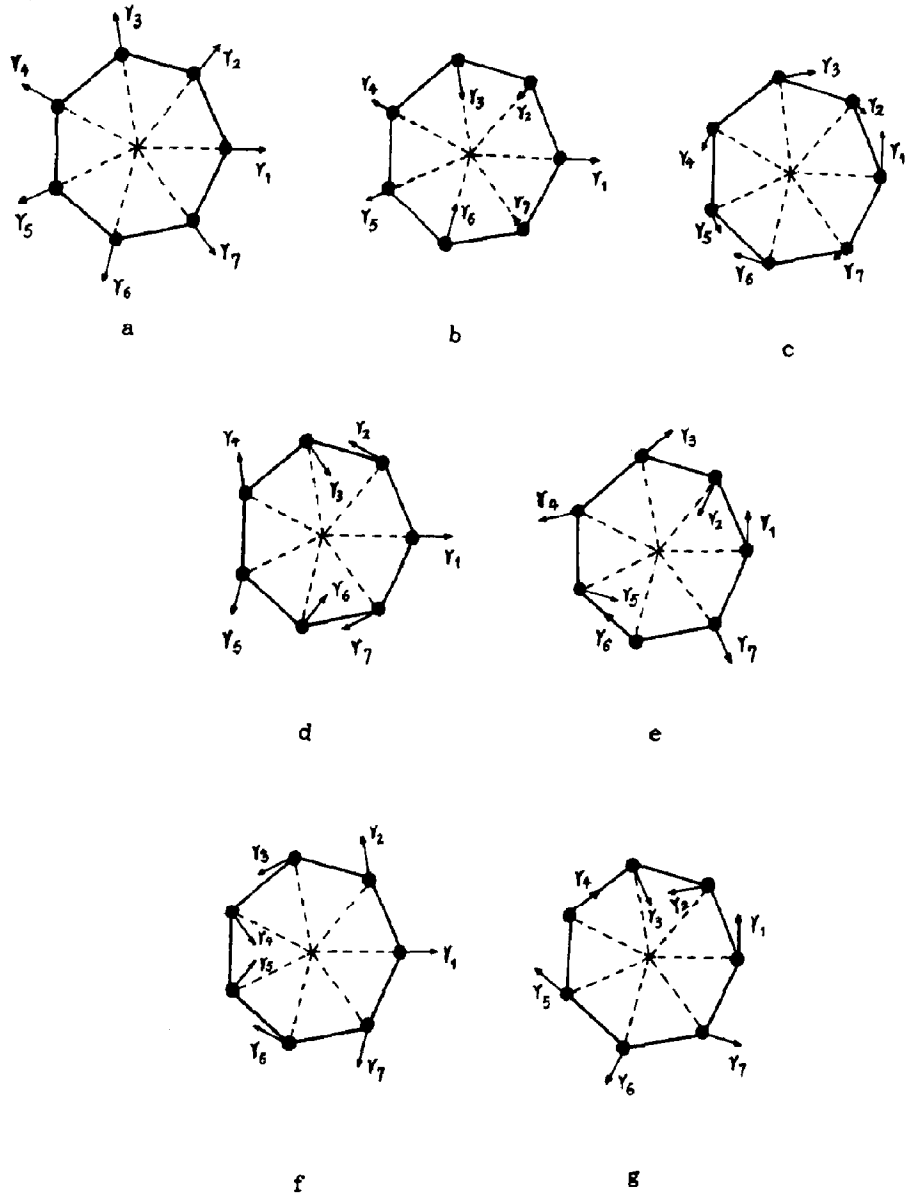

Fig. 4. The vibrational normal modes of our model in which the modes $a-g$ correspond to Q_1-Q_7, respectively.

man effect. See Table 1, the symmetry species associated with the polarizability components are A_1', E_1'', and E_2'. By reference to eq. (7), we have

$$D_{\text{Ram}} = A_1' + 2E_2'. \tag{8}$$

It is seen that there are five Raman active normal modes in the model shown in Fig. 2, but any two vibrations forming a pair of species E_2' must have the same frequency because they are "mixed" on transformation. There are two such pairs in (8). Consequently, the group-theoretical treatment predicts that our model will have three Raman active normal frequencies, one single and two doubly degenerate.

On the other hand, we are interested in the infrared active normal modes of our model as well. The modes having the symmetry associated with the three translations are infrared allowed [18]. We have mentioned that the symmetry species A_2'' and E_1' are associated with the three translations. By reference to (7), we have

$$D_{\text{infra}} = E_1'. \tag{9}$$

Therefore, one frequency of species E_1', which is doubly degenerate, will occur in the infrared spectrum.

In the following sections, we only calculate the frequencies of the Raman active normal modes (8) and the infrared active normal modes (9), and compare our results with observed values.

5. The vibrational normal coordinates

To obtain the seven vibrational normal coordinates of the species A_2', $2E_2'$ and E_1', we must use the projection operators and the irreducible representations of A_1', E_2', and E_1'. As an example, the derivation of the normal coordinate which belongs to the symmetry species, A_1' is given in Appendix A. The irreducible representations E_2' and E_1' are listed in Appendix B. Here, we directly write out the expressions of these normal coordinates.

5.1 The Raman active normal modes

The symmetry species of the Raman active normal modes have been given in eq. (8). The vibrational normal coordinate with symmetry A_1' is (see Appendix A)

$$\begin{aligned} Q_1 = e_1 &+ \left(\cos\frac{2\pi}{7}e_4 + \sin\frac{2\pi}{7}e_5\right) \\ &+ \left(\cos\frac{4\pi}{7}e_7 + \sin\frac{4\pi}{7}e_8\right) \\ &+ \left(\cos\frac{6\pi}{7}e_{10} + \sin\frac{6\pi}{7}e_{11}\right) \\ &+ \left(\cos\frac{6\pi}{7}e_{13} - \sin\frac{6\pi}{7}e_{14}\right) \\ &+ \left(\cos\frac{4\pi}{7}e_{16} - \sin\frac{4\pi}{7}e_{17}\right) \\ &+ \left(\cos\frac{2\pi}{7}e_{19} - \sin\frac{2\pi}{7}e_{20}\right). \end{aligned} \tag{10}$$

Its vibrational mode is shown in Fig. 4(a), where $r_1 = r_2 = \ldots = r_7$. This is just the dominant low-frequency mode described in Chou's theory [17].

There are two pairs of normal modes with symmetry E_2', in which the two modes of each pair are degenerate. The two normal coordinates of the first pair with symmetry E_2' are

$$\begin{aligned} Q_2 = e_1 &+ \cos\frac{4\pi}{7}\left(\cos\frac{2\pi}{7}e_4 + \sin\frac{2\pi}{7}e_5\right) \\ &+ \cos\frac{6\pi}{7}\left(\cos\frac{4\pi}{7}e_7 + \sin\frac{4\pi}{7}e_8\right) \\ &+ \cos\frac{2\pi}{7}\left(\cos\frac{6\pi}{7}e_{10} + \sin\frac{6\pi}{7}e_{11}\right) \\ &+ \cos\frac{2\pi}{7}\left(\cos\frac{6\pi}{7}e_{13} - \sin\frac{6\pi}{7}e_{14}\right) \\ &+ \cos\frac{6\pi}{7}\left(\cos\frac{4\pi}{7}e_{16} - \sin\frac{4\pi}{7}e_{17}\right) \\ &+ \cos\frac{4\pi}{7}\left(\cos\frac{2\pi}{7}e_{19} - \sin\frac{2\pi}{7}e_{20}\right), \end{aligned} \tag{11}$$

and

$$Q_3 = e_2 - \cos\frac{4\pi}{7}\left(\cos\frac{3\pi}{14}e_4 - \sin\frac{3\pi}{14}e_5\right) - \cos\frac{6\pi}{7}\left(\cos\frac{\pi}{14}e_7 + \sin\frac{\pi}{14}e_8\right) - \cos\frac{2\pi}{7}\left(\cos\frac{5\pi}{14}e_{10} + \sin\frac{5\pi}{14}e_{11}\right) + \cos\frac{2\pi}{7}\left(\cos\frac{5\pi}{14}e_{13} - \sin\frac{5\pi}{14}e_{14}\right) + \cos\frac{6\pi}{7}\left(\cos x\frac{\pi}{14}e_{16} - \sin\frac{\pi}{14}e_{17}\right) + \cos\frac{4\pi}{7}\left(\cos\frac{3\pi}{14}e_{19} + \sin\frac{3\pi}{14}e_{20}\right) \quad (12)$$

The vibrational modes of Q_2 and Q_3 are shown in Fig. 4(b) and (c), respectively, where

$$r_1 = r, \qquad r_2 = r_7 = |\cos\frac{4\pi}{7}|\, r,$$

$$r_3 = r_6 = |\cos\frac{6\pi}{7}|\, r,$$

and

$$r_4 = r_5 = \cos\frac{2\pi}{7}r.$$

Accordingly, the two normal coordinates of the second pair with symmetry E_2' are

$$Q_4 = e_1 - \left(\cos\frac{\pi}{7}e_4 - \sin\frac{\pi}{7}e_5\right) - \left(\cos\frac{5\pi}{7}e_7 + \sin\frac{5\pi}{7}e_8\right) - \left(\cos\frac{3\pi}{7}e_{10} - \sin\frac{3\pi}{7}e_{11}\right) - \left(\cos\frac{3\pi}{7}e_{13} + \sin\frac{3\pi}{7}e_{14}\right) - \left(\cos\frac{5\pi}{7}e_{16} - \sin\frac{5\pi}{7}e_{17}\right) - \left(\cos\frac{\pi}{7}e_{19} + \sin\frac{\pi}{7}e_{20}\right), \quad (13)$$

and

$$Q_5 = e_2 - \left(\cos\frac{5\pi}{14}e_4 + \sin\frac{5\pi}{14}e_5\right) + \left(\cos\frac{3\pi}{14}e_7 + \sin\frac{3\pi}{14}e_8\right) - \left(\cos\frac{\pi}{14}e_{10} + \sin\frac{\pi}{14}e_{11}\right) + \left(\cos\frac{\pi}{14}e_{13} - \sin\frac{\pi}{14}e_{14}\right) - \left(\cos\frac{3\pi}{14}e_{16} - \sin\frac{3\pi}{14}e_{17}\right) + \left(\cos\frac{5\pi}{14}e_{19} - \sin\frac{5\pi}{14}e_{20}\right). \quad (14)$$

The vibrational modes of Q_4 and Q_5 are shown in Fig. 4(d) and (e), respectively, where $r_1 = r_2 = \ldots = r_7$.

Now we have obtained the normal coordinates of the five Raman active normal modes, Q_1–Q_5, where Q_2 and Q_3 are degenerate, as well as Q_4 and Q_5. Therefore, as we mentioned in Section 4, a structure with the symmetry of group D_{7h} will have three Raman active normal frequencies.

5.2 *The infrared active normal coordinates*

According to the analysis in Section 4, our model, as depicted Fig. 2, will have two degenerate infrared normal modes which belong to the symmetry E_1'. The vibrational coordinates of these two normal modes are

$$Q_6 = e_1 + \left(\cos\frac{4\pi}{7}e_4 + \sin\frac{4\pi}{7}e_5\right) + \left(\cos\frac{6\pi}{7}e_7 - \sin\frac{6\pi}{7}e_8\right) + \left(\cos\frac{2\pi}{7}e_{10} - \sin\frac{2\pi}{7}e_{11}\right) + \left(\cos\frac{2\pi}{7}e_{13} + \sin\frac{2\pi}{7}e_{14}\right) + \left(\cos\frac{6\pi}{7}e_{16} + \sin\frac{6\pi}{7}e_{17}\right) + \left(\cos\frac{4\pi}{7}e_{19} - \sin\frac{4\pi}{7}e_{20}\right), \quad (15)$$

and

$$Q_7 = e_2 - \left(\cos\frac{\pi}{14}e_4 + \sin\frac{\pi}{14}e_5\right) - \left(\cos\frac{9\pi}{14}e_7 + \sin\frac{9\pi}{14}e_8\right) + \left(\cos\frac{3\pi}{14}e_{10} + \sin\frac{3\pi}{14}e_{11}\right) - \left(\cos\frac{3\pi}{14}e_{13} - \sin\frac{3\pi}{14}e_{14}\right) + \left(\cos\frac{9\pi}{14}e_{16} - \sin\frac{9\pi}{14}e_{17}\right) + \left(\cos\frac{\pi}{14}e_{19} - \sin\frac{\pi}{14}e_{20}\right). \quad (16)$$

The vibrational modes of Q_6 and Q_7 are shown in Fig. 4(f) and (g), respectively, where $r_1 = r_2 = \ldots = r_7$. These two modes have the same frequency.

So far, we have obtained all the Raman active and the infrared active normal coordinates of the present model. Next, we will calculate the vibrational frequencies of these normal modes under certain approximations.

6. The normal mode frequencies

Each of the V_L- and C_{HL}-barrels can be modeled as presented in Fig. 2. In this section, we will derive the expressions of frequency for the normal modes Q_1–Q_7 and calculate the normal frequencies of V_L- and C_{HL}-barrels in an IgG molecule by using these expressions.

Refer to Ref. [17]. Suppose the mass of each strand in Fig. 2 is m, the number of hydrogen bonds between any two neighboring strands is λ, and the stretching force constant of each hydrogen bond is k^s.

Figure 4(a) is the vibrational mode of the coordinate Q_1. Chou mainly considered this mode and called it the "dominant low-frequency normal mode" of a β-barrel structure [17]. When our model system vibrates in this mode, only the length of each hydrogen bond changes, while the seven interbond angles do not change, the potential energy of the system is only related to the stretching of the hydrogen bonds.

Let $r_i = r$, $i = 1, 2, \ldots, 7$; then the kinetic energy of the mode Q_1 is

$$T_1 = 7 \times \tfrac{1}{2} \times m\dot{r}^2, \quad (17)$$

where $\dot{r}$ denotes the derivative of first order with respect to time t.

From Fig. 4(a) we can see that the length change of each hydrogen bond is $2r \cos 5\pi/14$. So, according to Hooke's Law, the potential energy of the mode Q_1 can be written as

$$V_1 = 7 \times \tfrac{1}{2}(\lambda k^s)\left(2r \cos\frac{5\pi}{14}\right)^2 = 14\lambda k^s \sin^2\frac{\pi}{7}. \quad (18)$$

Substituting eqs. (17) and (18) into the following Lagrangian equation

$$\frac{\partial}{\partial t}\left(\frac{\partial L}{\partial \dot{r}}\right) - \frac{\partial L}{\partial r} = 0, \quad (19)$$

where $L = T_1 - V_1$. We obtain the vibrational equation of this mode

$$7m\ddot{r} + \left(28\lambda k^s \sin^2\frac{\pi}{7}\right)r = 0, \quad (20)$$

where $\ddot{r}$ denotes the derivative of second order with respect to time t.

Obviously, the vibrational frequency of this mode is

$$\omega_1 = \sqrt{\frac{28\lambda k^s \sin^2\frac{\pi}{7}}{7m}} = 2\sin\frac{\pi}{7}\sqrt{\frac{\lambda k^s}{m}}. \quad (21)$$

Using the wave number to express this frequency, we have

$$\tilde{\nu}_1 = \frac{\omega_1}{2\pi c} = \frac{1}{\pi c}\left(\sin\frac{\pi}{7}\right)\sqrt{\frac{\lambda k^s}{m}}. \quad (22)$$

This result is just the same as eq. (47) of Ref. [17], where it is obtained by the method of energy conservation.

In fact, the normal section of a V_L- or a C_{HL}-barrel is not a regular heptagon. Referring to Ref. [17], we extend eq. (22) to the following

equation which approximately deals with a irregular β-barrel with 7 strands:

$$\tilde{\nu}_1 = \frac{1}{\pi c}\left(\sin\frac{\pi}{7}\right)\sqrt{\frac{\Lambda k^s}{M}}\,. \tag{23}$$

where Λ is the total number of hydrogen bonds in the β-barrel, and M its total mass.

When the model system vibrates in the other modes in Fig. 4, both the length of each hydrogen bond and the interbond angles change. Therefore, the potential functions of these modes are related to both the stretching and bending of the hydrogen bonds. To obtain the expressions for the potential energy of these modes, we will use the approximation of valence forces [18] and some other approximations. The concrete methods of our approximations are given in Appendix C.

Now we turn to the mode Q_2 (Fig. 4b).

The kinetic energy of mode Q_2 is:

$$\begin{aligned} T_2 &= \sum_{i=1}^{7} \tfrac{1}{2} m \dot{r}_i^2 \\ &= \tfrac{1}{2} m \dot{r}^2 + 2 \times \tfrac{1}{2} m \left(\cos\frac{4\pi}{7}\dot{r}\right)^2 \\ &\quad + 2 \times \tfrac{1}{2} m \left(\cos\frac{6\pi}{7}\dot{r}\right)^2 \\ &\quad + 2 \times \tfrac{1}{2} m \left(\cos\frac{2\pi}{7}\dot{r}\right)^2 = \tfrac{7}{4} m \dot{r}^2. \end{aligned} \tag{24}$$

According to the approximation of valence forces (see Appendix C), the potential energy of this mode can be written as

$$\begin{aligned} V_2 &= \tfrac{1}{2}(\lambda k^s)\left(s_{12}^2 + s_{23}^2 + s_{34}^2 + s_{45}^2 + s_{56}^2 + s_{67}^2 + s_{71}^2\right) \\ &\quad + \tfrac{1}{2}(\lambda k^\alpha)\left(\alpha_{123}^2 + \alpha_{234}^2 + \alpha_{345}^2 + \alpha_{456}^2 + \alpha_{567}^2 \right. \\ &\quad \left. + \alpha_{671}^2 + \alpha_{712}^2\right), \end{aligned} \tag{25}$$

where s_{ij} $(i, j = 1, 2, \ldots, 7)$ is the extension of the H-bond between the strand i and j, α_{ijk} $(i, j, k = 1, 2, \ldots, 7)$ is the distortion of the valence angle between lines ij and jk, k^α is the force constant relating to the distortions of the valence angle, and k^s, as we have used, is the stretching force constant of a H-bond.

Using the methods given in Appendix C, we have

$$\begin{aligned} s_{12} &= s_{71} = \left(1 - \left|\cos\frac{4\pi}{7}\right|\right) r \cos\frac{5\pi}{14} \\ s_{23} &= s_{67} = \left(\left|\cos\frac{4\pi}{7}\right| + \left|\cos\frac{6\pi}{7}\right|\right) r \cos\frac{5\pi}{14} \\ s_{34} &= s_{56} = \left(\left|\cos\frac{6\pi}{7}\right| - \cos\frac{2\pi}{7}\right) r \cos\frac{5\pi}{14} \\ s_{45} &= 2\cos\frac{2\pi}{7} r \cos\frac{5\pi}{14} \end{aligned} \tag{26}$$

and

$$\begin{aligned} \alpha_{123} = \alpha_{671} &= \frac{1}{l}\left[\left(1 + \left|\cos\frac{4\pi}{7}\right|\right)\right. \\ &\quad \left. - \left(\left|\cos\frac{6\pi}{7}\right| - \left|\cos\frac{4\pi}{7}\right|\right)\right] r \sin\frac{5\pi}{14}, \\ \alpha_{234} = \alpha_{567} &= \frac{1}{l}\left[\left(\left|\cos\frac{6\pi}{7}\right| - \left|\cos\frac{4\pi}{7}\right|\right)\right. \\ &\quad \left. + \left(\left|\cos\frac{6\pi}{7}\right| + \cos\frac{2\pi}{7}\right)\right] r \sin\frac{5\pi}{14}, \\ \alpha_{345} = \alpha_{456} &= \frac{1}{l}\left(\left|\cos\frac{6\pi}{7}\right| + \cos\frac{2\pi}{7}\right) r \sin\frac{5\pi}{14}, \\ \alpha_{712} &= \frac{2}{l}\left(1 + \left|\cos\frac{4\pi}{7}\right|\right) r \sin\frac{5\pi}{14}, \end{aligned} \tag{27}$$

where l is the equilibrium distance between any two neighbouring strands.

Substituting eqs. (27) and (26) into (25), we have

$$\begin{aligned} V_2 &= \tfrac{1}{2}\lambda k^s\left(9 + 4\cos\frac{6\pi}{7} + 4\cos\frac{2\pi}{7} + 11\cos\frac{4\pi}{7}\right) \\ &\quad \times \left(\cos^2\frac{5\pi}{14}\right) r^2 \\ &\quad + \tfrac{1}{2}\lambda\frac{k^\alpha}{l^2}\left(21 + 7\cos\frac{6\pi}{7} - 28\cos\frac{4\pi}{7}\right) \\ &\quad \times \left(\sin^2\frac{5\pi}{14}\right) r^2. \end{aligned} \tag{28}$$

We can obtain the vibrational equation of mode Q_2 by substituting $L = T_2 - V_2$ into the La-

grangian equation (19). Then the vibrational frequency of mode Q_2 can be easily written out

$$\tilde{\nu}_2 = \frac{1}{\pi c}\left\{\frac{\lambda}{14m}\left[k^s\left(9 + 4\cos\frac{6\pi}{7} + 4\cos\frac{2\pi}{7} + 11\cos\frac{4\pi}{7}\right)\cos^2\frac{5\pi}{14} + \frac{k^\alpha}{l^2}\left(21 + 7\cos\frac{6\pi}{7} - 28\cos\frac{4\pi}{7}\right)\times\sin^2\frac{5\pi}{14}\right]\right\}^{1/2} \quad (29)$$

Similarly, the kinetic energy, the potential energy, and the vibrational frequency of the mode Q_3 (Fig. 4c) can be obtained, as given by the following equations:

$$T_3 = T_2 = \tfrac{7}{4}m\dot{r}^2, \quad (30)$$

$$V_3 = \tfrac{7}{2}\lambda\left[k^s\left(1 - \cos\frac{4\pi}{7}\right)\sin^2\frac{5\pi}{14} + \frac{k^\alpha}{l^2}\left(1 - \cos\frac{6\pi}{7}\right)\cos^2\frac{5\pi}{14}\right]r^2, \quad (31)$$

and

$$\tilde{\nu}_3 = \frac{1}{2\pi c}\left\{\frac{2\lambda}{m}\left[k^s\left(1 - \cos\frac{4\pi}{7}\right)\times\sin^2\frac{5\pi}{14} + \frac{k^\alpha}{l^2}\left(1 - \cos\frac{6\pi}{7}\right)\sin^2\frac{5\pi}{14}\right]\right\}^{1/2}, \quad (32)$$

The vibrational normal modes Q_2 and Q_3 are degenerate. These two modes must have the same frequency, i.e.

$$\tilde{\nu}_2 = \tilde{\nu}_3. \quad (33)$$

The value of the stretching force constant of a H-bond is [19]

$$k^s = 0.13 \text{ mdyn/Å}. \quad (34)$$

Substituting k^s and the expressions (29) and (32) into (33), we have

$$k^\alpha/l^2 = 0.05 \text{ mdyn/Å}. \quad (35)$$

Considering the nonregularity of the real β-barrel, and under the conditions of (34) and (35), we extend eq. (29) to the following form

$$\tilde{\nu}_2 = \tilde{\nu}_3 = \frac{1}{\pi c}\left\{\frac{\Lambda}{14M}\left[k^s\left(9 + 4\cos\frac{6\pi}{7} + 4\cos\frac{2\pi}{7} + 11\cos\frac{4\pi}{7}\right)\cos^2\frac{5\pi}{14} + \frac{k^\alpha}{l^2}\left(21 + 7\cos\frac{6\pi}{7} - 28\cos\frac{4\pi}{7}\right)\times\sin^2\frac{5\pi}{14}\right]\right\}^{1/2} \quad (36)$$

For the vibrational modes Q_4 and Q_5, we have

$$T_4 = T_5 = \tfrac{7}{2}m\dot{r}^2, \quad (r_i = r,\ i = 1, 2, \ldots, 7) \quad (37)$$

$$V_4 = V_5 = \tfrac{7}{2}\lambda\left[k^s\left(1 - \cos\frac{6\pi}{7}\right) + \frac{k^\alpha}{l^2}\left(2 + \cos\frac{2\pi}{7} - \cos\frac{4\pi}{7} - 2\cos\frac{6\pi}{7}\right)\right]r^2 \quad (38)$$

and

$$\tilde{\nu}_4 = \tilde{\nu}_5 = \frac{1}{2\pi c}\left\{\frac{\Lambda}{M}\left[k^s\left(1 - \cos\frac{6\pi}{7}\right) + \frac{k^\alpha}{l^2}\left(2 + \cos\frac{2\pi}{7} - \cos\frac{4\pi}{7} - 2\cos\frac{6\pi}{7}\right)\right]\right\}^{1/2} \quad (39)$$

Finally, for the degenerate infrared active modes Q_6 and Q_7, we have

$$T_6 = T_7 = \tfrac{7}{2}m\dot{r}^2, \quad (r_i = r,\ i = 1, 2, \ldots, 7) \quad (40)$$

$$V_6 = V_7 = \tfrac{7}{2}\lambda\left[k^s\left(1 - \cos\frac{4\pi}{7}\right) + \frac{k^\alpha}{l^2}\left(2 - \cos\frac{2\pi}{7} - 2\cos\frac{4\pi}{7} + \cos\frac{6\pi}{7}\right)\right]r^2, \quad (41)$$

Table 2

Vibrational frequencies of V_L- and C_{HL}-barrels in the normal modes Q_1–Q_7

Species	Active in	Mode	Frequency (cm^{-1})	
			V_L-barrel	C_{HL}-barrel
A_1'	Raman	Q_1	35.8 [a]	28.6 [a]
E_2'	Raman	Q_2, Q_3	60.6	48.4
		Q_4, Q_5	79.0	63.0
E_1'	Infrared	Q_6, Q_7	51.8	41.4

[a] The value obtained by Chou as a dominant frequency in Ref. [17].

$$\tilde{\nu}_6 = \tilde{\nu}_7 = \frac{1}{2\pi c}\left\{\frac{\Lambda}{M}\left[k^s\left(1-\cos\frac{4\pi}{7}\right) + \frac{k^\alpha}{l^2}\left(1-\cos\frac{2\pi}{7}-2\cos\frac{4\pi}{7} + \cos\frac{6\pi}{7}\right)\right]\right\}^{1/2} \quad (42)$$

So far, we have obtained the expressions for calculating the frequencies of the modes Q_1–Q_7. Now we concretely calculate the frequencies of the V_L- and C_{HL}-barrels in these vibrational modes.

There are two V_L-barrels in an IgG molecule. For this type of β-barrel, we have [16] $M \approx 5440$ g/N and $\Lambda = 42$, where $N = 6.02\ 10^{23}$ is the Avogadro constant. For a C_{HL}-barrel, we have $M \approx 7104$ g/N and $\Lambda = 35$. Substituting these data and eqs. (34) into expressions (21), (36), (39) and (42), we may obtain the frequencies of these two types of β-barrel in these vibrational modes. We have listed the results in Table 2.

In the next section, we shall discuss some parameters and compare our theoretical results with the experimental data.

7. Discussion and conclusions

There are two force constants k^s and k^α/l^2 in this paper. $k^s = 0.13$ mdyn/Å is the stretching force constant of a H-bond [19]. Considering $\tilde{\nu}_2 = \tilde{\nu}_3$, we obtained $k^\alpha/l^2 = 0.05$ mdyn/Å. In fact, Q_2 and Q_3 are degenerate. This type of degeneracy arises because of the presence of the seven-fold axis of symmetry in our model, and is quite independent of numerical values of the force constant or masses. But to calculate this doubly degenerate frequency, we must to some approximations and neglect some interactions, which make the frequency be related to the numerical values of k^s and k^α/l^2. The force constant k^α/l^2 is mainly associated with the bending of a H-bond. Ref. [19] gave the bending force constant of a H-bond $k^b = 0.03$ mdyn/Å. It is seen that the numerical value of k^α/l^2 in our model is quite close to this value and thus is reasonable.

In Table 2, we have listed the fundamental frequencies of V_L- and C_{HL}-barrels in and IgG molecule, which are Raman or infrared active.

The Raman spectrum of an IgG molecule was obtained by Painter et al. [3]. In this spectrum, there are two lines clearly resolved at 28 and 36 cm^{-1}, and a third appearing as a weak shoulder near 60 cm^{-1}. From Table 2 we find that the strong lines of 28 and 36 cm^{-1} are corresponding to the normal modes Q_1 (C_{HL}) and Q_1 (V_L), respectively. When a β-barrel vibrates in mode Q_1, it has the lowest normal frequency. Therefore, the breathing motion mode Q_1 is the dominant low-frequency mode of a β-barrel. The peak near 60 cm^{-1} in the spectrum may result from the modes $Q_{2,3}$ (V_L) and $Q_{4,5}$ (C_{HL}). Observing the spectrum of Ref. [3] carefully, we find also exist small crownings between 45–55 cm^{-1}, which are indiscernible due to the higher background [5]. We think that some of these small crownings may be corresponding to Raman modes, and the one near 50 cm^{-1} may be contributable to the modes $Q_{2,3}$ (C_{HL}). The Raman modes $Q_{4,5}$ (V_L) lie out of this observed range.

In Ref. [16], Chou also calculated the dominant low-frequency of a V_L-barrel which is 28.3 cm^{-1}. In an IgG molecule, there are 10 β-barrels (two V_H-barrels and eight C_{HL}-barrels) that can generate the frequency mode about 28 cm^{-1}. That is why the peak of 28 cm^{-1} is the strongest one in the spectrum.

So far, no infrared spectrum of an IgG molecule is obtained. According to our calculation we predict that at least two lines at about 51 and 41 cm^{-1} will occur in the infrared spectrum (see Table 2).

Based on Chou's quasi-continuity model, we have obtained the Raman and the infrared active normal modes of the V_L- and C_{HL}-barrels in an IgG molecule with the method of group theory. The Raman fundamental frequencies we obtained are in good agreement with the experimental values. With the same method, we can also calculate the normal modes of other β-barrel proteins. For example, there is a β-barrel with 14-strands in the molecule Concanavalin A. In its Raman spectrum, there are several weak peaks around 20 cm^{-1} [5]. Using the quasi-continuity model and Chou's formula [17], one can only obtain the dominant frequency about 20 cm^{-1}. But using the method presented in this paper, we can also get the other Raman modes. Therefore, our work may improve and complete Chou's quasi-continuity model.

Appendix A

We explain here how to obtain the normal coordinate Q_1 of species A_1'.

Applying the projection operator $\hat{p}^{A_1'}$ to e_1, we can get

$$\hat{p}^{A_1'}e_1 = \frac{d'_{A1}}{g}\sum_R \chi^*_{A_1'}(R)\hat{R}e_1, \tag{A.1}$$

where $d_{A_1'} = 1$ is the dimension of the irreducible representation A_1', $g = 28$ is the number of the operations in the group D_{7h}, $\hat{R}$ represents any operation in D_{7h}, $\chi^*_{A_1'}(R)$ is the complex conjugate of the character of A_1' for operation R, and the sum is over all these operations.

We can see from Table 1 that, for any operation R, there is

$$\chi^*_{A_1'}(R) = 1. \tag{A.2}$$

Applying the operations of group D_{7h} to e_1, we have

$$\begin{aligned}
Ee_1 &= C_2'^{(1)}e_1 = \sigma_h e_1 = \sigma_v^{(1)}e_1 = e_1\\
C_7e_1 &= C_2'^{(5)}e_1 = S_7e_1 = \sigma_v^{(5)}e_1\\
&= \cos\frac{2\pi}{7}e_4 + \sin\frac{2\pi}{7}e_5\\
C_7^2e_1 &= C_2'^{(2)}e_1 = S_7^2e_1 = \sigma_v^{(2)}e_1\\
&= \cos\frac{4\pi}{7}e_7 + \sin\frac{4\pi}{7}e_8\\
C_7^3e_1 &= C_2'^{(6)}e_1 = S_7^3e_1 = \sigma_v^{(6)}e_1\\
&= \cos\frac{6\pi}{7}e_{10} + \sin\frac{6\pi}{7}e_{11}\\
C_7^4e_1 &= C_2'^{(3)}e_1 = S_7^4e_1 = \sigma_v^{(3)}e_1\\
&= \cos\frac{6\pi}{7}e_{13} - \sin\frac{6\pi}{7}e_{14}\\
C_7^5e_1 &= C_2'^{(7)}e_1 = S_7^5e_1 = \sigma_v^{(7)}e_1\\
&= \cos\frac{4\pi}{7}e_{16} - \sin\frac{4\pi}{7}e_{17}\\
C_7^6e_1 &= C_2'^{(4)}e_1 = S_7^6e_1 = \sigma_v^{(4)}e_1\\
&= \cos\frac{2\pi}{7}e_{19} - \sin\frac{2\pi}{7}e_{20}
\end{aligned} \tag{A.3}$$

Substituting eqs. (A.2) and (A.3) into (A.1), we have

$$\begin{aligned}
\hat{p}^{A_1'}e_1 = \tfrac{1}{28}\times 4\Bigg[&e_1 + \left(\cos\frac{2\pi}{7}e_4 + \sin\frac{2\pi}{7}e_5\right)\\
&+ \left(\cos\frac{4\pi}{7}e_7 + \sin\frac{4\pi}{7}e_8\right)\\
&+ \left(\cos\frac{6\pi}{7}e_{10} + \sin\frac{6\pi}{7}e_{11}\right)\\
&+ \left(\cos\frac{6\pi}{7}e_{13} - \sin\frac{6\pi}{7}e_{14}\right)\\
&+ \left(\cos\frac{4\pi}{7}e_{16} - \sin\frac{4\pi}{7}e_{17}\right)\\
&+ \left(\cos\frac{2\pi}{7} - \sin\frac{2\pi}{7}e_{20}\right)\Bigg]
\end{aligned} \tag{A.4}$$

The displacement in the right hand of eq. (A.4) keep the centroid of the system stationary.

Therefore, the normal coordinate of species A_1' can be written as

$$Q_1 = e_1 + \left(\cos\frac{2\pi}{7}e_4 + \sin\frac{2\pi}{7}e_5\right) + \left(\cos\frac{4\pi}{7}e_7 + \sin\frac{4\pi}{7}e_8\right) + \left(\cos\frac{6\pi}{7}e_{10} + \sin\frac{6\pi}{7}e_{11}\right) + \left(\cos\frac{6\pi}{7}e_{13} - \sin\frac{6\pi}{7}e_{14}\right) + \left(\cos\frac{4\pi}{7}e_{16} - \sin\frac{4\pi}{7}e_{17}\right) + \left(\cos\frac{2\pi}{7}e_{10} - \sin\frac{2\pi}{7}e_{20}\right). \quad \text{(A.5)}$$

To obtain the normal coordinates of species E_2' and E_1', we must use the two-dimensional representation matrixes of E_2' and E_1'. The derivations of Q_2–Q_7 are little more complex than that of Q_1. We only list the irreducible representations E_2' and E_1' in Appendix B. To deeply understand the projection operators and how to use them to obtain the vibrational normal coordinates, please see Ref. [20].

Appendix B

Table B1
The irreducible representation E_2'

E		C_7		C_7^6		C_7^2		C_7^5		C_7^3	
1	0	$\cos\frac{4\pi}{7}$	$-\frac{1}{2}\sin\frac{4\pi}{7}$	$\cos\frac{4\pi}{7}$	$\frac{1}{2}\sin\frac{4\pi}{7}$	$\cos\frac{6\pi}{7}$	$\frac{1}{2}\sin\frac{6\pi}{7}$	$\cos\frac{6\pi}{7}$	$-\frac{1}{2}\sin\frac{6\pi}{7}$	$\cos\frac{2\pi}{7}$	$\frac{1}{2}\sin\frac{2\pi}{7}$
0	1	$2\sin\frac{4\pi}{7}$	$\cos\frac{4\pi}{7}$	$-2\sin\frac{4\pi}{7}$	$\cos\frac{4\pi}{7}$	$-2\sin\frac{6\pi}{7}$	$\cos\frac{6\pi}{7}$	$2\sin\frac{6\pi}{7}$	$\cos\frac{6\pi}{7}$	$-2\sin\frac{2\pi}{7}$	$\cos\frac{2\pi}{7}$
C_7^4		$C_2'^{(1)}$		$C_2'^{(2)}$		$C_2'^{(3)}$		$C_2'^{(4)}$		$C_2'^{(5)}$	
$\cos\frac{2\pi}{7}$	$-\frac{1}{2}\sin\frac{2\pi}{7}$	1	0	$\cos\frac{6\pi}{7}$	$-\frac{1}{2}\sin\frac{6\pi}{7}$	$\cos\frac{2\pi}{7}$	$\frac{1}{2}\sin\frac{2\pi}{7}$	$\cos\frac{4\pi}{7}$	$-\frac{1}{2}\sin\frac{4\pi}{7}$	$\cos\frac{4\pi}{7}$	$\frac{1}{2}\sin\frac{4\pi}{7}$
$2\sin\frac{2\pi}{7}$	$\cos\frac{2\pi}{7}$	0	−1	$-2\sin\frac{6\pi}{7}$	$-\cos\frac{6\pi}{7}$	$2\sin\frac{2\pi}{7}$	$-\cos\frac{2\pi}{7}$	$-2\sin\frac{4\pi}{7}$	$-\cos\frac{4\pi}{7}$	$2\sin\frac{4\pi}{7}$	$-\cos\frac{4\pi}{7}$
$C_2'^{(6)}$		$C_2'^{(7)}$		σ_h		S_7		S_7^6		S_7^2	
$\cos\frac{2\pi}{7}$	$-\frac{1}{2}\sin\frac{2\pi}{7}$	$\cos\frac{6\pi}{7}$	$\frac{1}{2}\sin\frac{6\pi}{7}$	1	0	$\cos\frac{4\pi}{7}$	$-\frac{1}{2}\sin\frac{4\pi}{7}$	$\cos\frac{4\pi}{7}$	$\frac{1}{2}\sin\frac{4\pi}{7}$	$\cos\frac{6\pi}{7}$	$\frac{1}{2}\sin\frac{6\pi}{7}$
$-2\sin\frac{2\pi}{7}$	$-\cos\frac{2\pi}{7}$	$2\sin\frac{6\pi}{7}$	$-\cos\frac{6\pi}{7}$	0	1	$2\sin\frac{4\pi}{7}$	$\cos\frac{4\pi}{7}$	$-2\sin\frac{4\pi}{7}$	$\cos\frac{4\pi}{7}$	$-2\sin\frac{6\pi}{7}$	$\cos\frac{6\pi}{7}$
S_7^5		S_7^3		S_7^4		$\sigma_v^{(1)}$		$\sigma_v^{(2)}$		$\sigma_v^{(3)}$	
$\cos\frac{6\pi}{7}$	$-\frac{1}{2}\sin\frac{6\pi}{7}$	$\cos\frac{2\pi}{7}$	$\frac{1}{2}\sin\frac{2\pi}{7}$	$\cos\frac{2\pi}{7}$	$-\frac{1}{2}\sin\frac{2\pi}{7}$	1	0	$\cos\frac{6\pi}{7}$	$-\frac{1}{2}\sin\frac{6\pi}{7}$	$\cos\frac{2\pi}{7}$	$\frac{1}{2}\sin\frac{2\pi}{7}$
$2\sin\frac{6\pi}{7}$	$\cos\frac{6\pi}{7}$	$-2\sin\frac{2\pi}{7}$	$\cos\frac{2\pi}{7}$	$2\sin\frac{2\pi}{7}$	$\cos\frac{2\pi}{7}$	0	−1	$-2\sin\frac{6\pi}{7}$	$-\cos\frac{6\pi}{7}$	$2\sin\frac{2\pi}{7}$	$-\cos\frac{2\pi}{7}$
$\sigma_v^{(4)}$		$\sigma_v^{(5)}$		$\sigma_v^{(6)}$		$\sigma_v^{(7)}$					
$\cos\frac{4\pi}{7}$	$-\frac{1}{2}\sin\frac{4\pi}{7}$	$\cos\frac{4\pi}{7}$	$\frac{1}{2}\sin\frac{4\pi}{7}$	$\cos\frac{2\pi}{7}$	$-\frac{1}{2}\sin\frac{2\pi}{7}$	$\cos\frac{6\pi}{7}$	$\frac{1}{2}\sin\frac{6\pi}{7}$				
$-2\sin\frac{4\pi}{7}$	$-\cos\frac{4\pi}{7}$	$2\sin\frac{4\pi}{7}$	$-\cos\frac{4\pi}{7}$	$-2\sin\frac{2\pi}{7}$	$-\cos\frac{2\pi}{7}$	$2\sin\frac{6\pi}{7}$	$-\cos\frac{6\pi}{7}$				

Note: Each square represents a matrix. For example:

$$E_2'(E)=\begin{bmatrix}1 & 0\\ 0 & 1\end{bmatrix}.$$

Table B2

The irreducible representation E_1'

E	C_7	C_7^6	C_7^2	C_7^5	C_7^3
$\begin{matrix}1 & 0\\ 0 & 1\end{matrix}$	$\begin{matrix}\cos\frac{2\pi}{7} & -\sin\frac{2\pi}{7}\\ \sin\frac{2\pi}{7} & \cos\frac{2\pi}{7}\end{matrix}$	$\begin{matrix}\cos\frac{2\pi}{7} & \sin\frac{2\pi}{7}\\ -\sin\frac{2\pi}{7} & \cos\frac{2\pi}{7}\end{matrix}$	$\begin{matrix}\cos\frac{4\pi}{7} & -\sin\frac{4\pi}{7}\\ \sin\frac{4\pi}{7} & \cos\frac{4\pi}{7}\end{matrix}$	$\begin{matrix}\cos\frac{4\pi}{7} & \sin\frac{4\pi}{7}\\ -\sin\frac{4\pi}{7} & \cos\frac{4\pi}{7}\end{matrix}$	$\begin{matrix}\cos\frac{6\pi}{7} & -\sin\frac{6\pi}{7}\\ \sin\frac{6\pi}{7} & \cos\frac{6\pi}{7}\end{matrix}$
C_7^4	$C_2'^{(1)}$	$C_2'^{(2)}$	$C_2'^{(3)}$	$C_2'^{(4)}$	$C_2'^{(5)}$
$\begin{matrix}\cos\frac{6\pi}{7} & \sin\frac{6\pi}{7}\\ -\sin\frac{6\pi}{7} & \cos\frac{6\pi}{7}\end{matrix}$	$\begin{matrix}1 & 0\\ 0 & -1\end{matrix}$	$\begin{matrix}\cos\frac{4\pi}{7} & \sin\frac{4\pi}{7}\\ \sin\frac{4\pi}{7} & -\cos\frac{4\pi}{7}\end{matrix}$	$\begin{matrix}\cos\frac{6\pi}{7} & \sin\frac{6\pi}{7}\\ -\sin\frac{6\pi}{7} & -\cos\frac{6\pi}{7}\end{matrix}$	$\begin{matrix}\cos\frac{2\pi}{7} & -\sin\frac{2\pi}{7}\\ -\sin\frac{2\pi}{7} & -\cos\frac{2\pi}{7}\end{matrix}$	$\begin{matrix}\cos\frac{2\pi}{7} & \sin\frac{2\pi}{7}\\ \sin\frac{2\pi}{7} & -\cos\frac{2\pi}{7}\end{matrix}$
$C_2'^{(6)}$	$C_2'^{(7)}$	σ_h	S_7	S_7^6	S_7^2
$\begin{matrix}\cos\frac{6\pi}{7} & \sin\frac{6\pi}{7}\\ \sin\frac{6\pi}{7} & -\cos\frac{6\pi}{7}\end{matrix}$	$\begin{matrix}\cos\frac{4\pi}{7} & -\sin\frac{4\pi}{7}\\ -\sin\frac{4\pi}{7} & -\cos\frac{4\pi}{7}\end{matrix}$	$\begin{matrix}1 & 0\\ 0 & 1\end{matrix}$	$\begin{matrix}\cos\frac{2\pi}{7} & -\sin\frac{2\pi}{7}\\ \sin\frac{2\pi}{7} & \cos\frac{2\pi}{7}\end{matrix}$	$\begin{matrix}\cos\frac{2\pi}{7} & \sin\frac{2\pi}{7}\\ -\sin\frac{2\pi}{7} & \cos\frac{2\pi}{7}\end{matrix}$	$\begin{matrix}\cos\frac{4\pi}{7} & -\sin\frac{4\pi}{7}\\ \sin\frac{4\pi}{7} & \cos\frac{4\pi}{7}\end{matrix}$
S_7^5	S_7^3	S_7^4	$\sigma_v^{(1)}$	$\sigma_v^{(2)}$	$\sigma_v^{(3)}$
$\begin{matrix}\cos\frac{4\pi}{7} & \sin\frac{4\pi}{7}\\ -\sin\frac{4\pi}{7} & \cos\frac{4\pi}{7}\end{matrix}$	$\begin{matrix}\cos\frac{6\pi}{7} & -\sin\frac{6\pi}{7}\\ \sin\frac{6\pi}{7} & \cos\frac{6\pi}{7}\end{matrix}$	$\begin{matrix}\cos\frac{6\pi}{7} & \sin\frac{6\pi}{7}\\ -\sin\frac{6\pi}{7} & \cos\frac{6\pi}{7}\end{matrix}$	$\begin{matrix}1 & 0\\ 0 & -1\end{matrix}$	$\begin{matrix}\cos\frac{4\pi}{7} & \sin\frac{4\pi}{7}\\ \sin\frac{4\pi}{7} & -\cos\frac{4\pi}{7}\end{matrix}$	$\begin{matrix}\cos\frac{6\pi}{7} & -\sin\frac{6\pi}{7}\\ -\sin\frac{6\pi}{7} & -\cos\frac{6\pi}{7}\end{matrix}$
$\sigma_v^{(4)}$	$\sigma_v^{(5)}$	$\sigma_v^{(6)}$	$\sigma_v^{(7)}$		
$\begin{matrix}\cos\frac{2\pi}{7} & -\sin\frac{2\pi}{7}\\ -\sin\frac{2\pi}{7} & -\cos\frac{2\pi}{7}\end{matrix}$	$\begin{matrix}\cos\frac{2\pi}{7} & \sin\frac{2\pi}{7}\\ \sin\frac{2\pi}{7} & -\cos\frac{2\pi}{7}\end{matrix}$	$\begin{matrix}\cos\frac{6\pi}{7} & \sin\frac{6\pi}{7}\\ \sin\frac{6\pi}{7} & -\cos\frac{6\pi}{7}\end{matrix}$	$\begin{matrix}\cos\frac{4\pi}{7} & -\sin\frac{4\pi}{7}\\ -\sin\frac{4\pi}{7} & -\cos\frac{4\pi}{7}\end{matrix}$		

Appendix C

We used the valence force approximation in Section 6 to write out the potential functions of the normal modes Q_2–Q_7. In this approximation, the forces considered are those which resist the extension or compression of the H-bonds, together with those which oppose the bending or torsion of H-bonds; forces between non-bonded strands are not directly considered. Figure 5 shows the motions of strands 1, 2 and 3 in mode Q_2. Here A, B and C denote the equilibrium positions of strands 1, 2 and 3, respectively. r_1, r_2 and r_3 are their respective displacement vector. In model Q_2, $r_1 = r$, $r_2 = |\cos 4\pi/7|\, r$ and $r_3 = |\cos 6\pi/7|\, r$. Let A_1, B_1 and C_1 be the vibrational positions of A, B and C, respectively. Here $\angle C_1CB = \angle CBB_1 = \angle B_1BA = 5\pi/14$, and $\angle BAA_1 = 9\pi/14$. According to the approximation of valence forces [18], the potential energy of the system in Fig. 5 can be written as

$$V = \tfrac{1}{2}\lambda k^s\left(s_{AB}^2 + s_{BC}^2\right) + \tfrac{1}{2}\lambda k^\alpha\left(\alpha_{ABC}\right)^2, \qquad \text{(C.1)}$$

where s_{AB} and s_{BC} are the extensions of the H-bonds between the strands A and B, and between the strands B and C, respectively. $\alpha_{ABC} = \angle A_1B_1C_1 - \angle ABC$ is the distortion of the valence angle ABC.

We think the stretching energy of the H-bonds between the strands A and B is mainly due to the stretching of the H-bonds along the direction of the line AB. Based on this viewpoint, we take

$$s_{AB} \approx r_1 \cos\frac{5\pi}{14} - r_2 \cos\frac{5\pi}{14} = \left(1 - \left|\cos\frac{4\pi}{7}\right|\right) r \cos\frac{5\pi}{14}. \qquad \text{(C.2)}$$

In the same way, we have

$$s_{BC} \approx r_2 \cos\frac{5\pi}{14} r_3 \cos\frac{5\pi}{14} = \left(\left|\cos\frac{4\pi}{7}\right| + \left|\cos\frac{6\pi}{7}\right|\right) r \cos\frac{5\pi}{14}. \qquad \text{(C.3)}$$

Translating the angle $A_1B_1C_1$ along the direction of $B_1 \rightarrow B$ (see Fig. 5), we obtain the angle

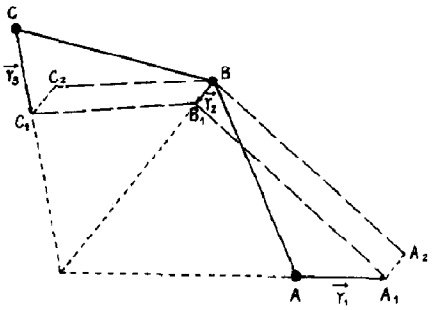

Fig. 5. The sketch map describing the motions of strands 1, 2 and 3 in mode Q_2.

A_2BC which equals to $\angle A_1B_1C_1$. Then

$$\alpha_{ABC} = \angle A_2BC_2 - \angle ABC = \angle A_2BA - \angle C_2BC, \qquad \text{(C.4)}$$

where $\angle A_2BA$ is the increase of the valence angle ABC produced by the motions of the strands A and B. $\angle A_2BA$ is mainly determined by the vertical components of r_1 and r_2 to the line AB. We may approximate the expression for $\angle A_2BA$ as

$$\angle A_2BA \approx \frac{1}{\overline{AB}}\left(r_1 \sin\frac{5\pi}{14} + r_2 \sin\frac{5\pi}{14}\right) = \frac{1}{l}\left(1 + \left|\cos\frac{4\pi}{7}\right|\right) r \sin\frac{5\pi}{14}, \qquad \text{(C.5)}$$

where $l = \overline{AB}$ is the equilibrium distance between the strands A and B.

Similarly, $\angle C_2BC$ is the decrease of the angle ABC produced by the motions of the strands B and C. With the same approximation mentioned above, we have

$$\angle C_2BC \approx \frac{1}{\overline{BC}}\left(r_3 \sin\frac{5\pi}{14} - r_2 \sin\frac{5\pi}{14}\right) = \frac{1}{l}\left(\left|\cos\frac{6\pi}{7}\right| - \left|\cos\frac{4\pi}{7}\right|\right) r \sin\frac{5\pi}{14}. \qquad \text{(C.6)}$$

By substituting eqs. (C.2)–(C.6) into (C.1), we obtain

$$V = \tfrac{1}{2}\lambda k^s \left[\left(1 - \left| \cos\frac{4\pi}{7} \right| \right)^2 + \left(\left| \cos\frac{4\pi}{7} \right| + \left| \cos\frac{6\pi}{7} \right| \right)^2 \right] r^2 \cos^2\frac{5\pi}{14} + \tfrac{1}{2}\lambda \frac{k^\alpha}{l^2} \left[\left(1 + \left| \cos\frac{4\pi}{7} \right| \right) - \left(\left| \cos\frac{6\pi}{7} \right| - \left| \cos\frac{4\pi}{7} \right| \right) \right]^2 r^2 \sin^2\frac{5\pi}{14}. \quad \text{(C.7)}$$

This is the potential function of the model in Fig. 5. In the same way, we can obtain the potential functions of modes Q_2–Q_7 which are given in Section 6.

Acknowledgments

We are grateful to Prof. Chun-Ting Zhang and Dr. Fu-Li Du for the helpful discussions during this study.

References

1 K.G. Brown, S.C. Erfurth, E.W. Small and W.L. Peticolas, Proc. Natl. Acad. Sci. U.S.A. 69 (1972) 1467.
2 L. Genzel, F. Keilman, T.P. Martin, G. Winterling, Y. Yacoby, H. Fröhlich and M.W. Makinen, Biopolymers 15 (1976) 219.
3 P.C. Painter and L.E. Mosher, Biopolymers 18 (1979) 3121.
4 P.C. Painter, L.E. Mosher and C. Rhoads, Biopolymers 20 (1981) 243.
5 P.C. Painter, L.E. Mosher and C. Rhoads, Biopolymers 21 (1982) 1469.
6 Y. Suezaki and N. Gō, Int. J. Peptide Protein Res. 7 (1975) 333.
7 T. Noguti and N. Gō, Nature 296 (1982) 776.
8 N. Gō, T. Noguti and T. Nishikawa, Proc. Natl. Acad. Sci. U.S.A. 80 (1983) 3696.
9 B. Brooks and M. Karplus, Proc. Natl. Acad. Sci. U.S.A. 80 (1982) 6571.
10 R.M. Levy, A.R. Srinirasam, W.K. Olson and J.A. McCammon, Biopolymers 23 (1984) 1099.
11 K.C. Chou, Biochem. J. 215 (1983) 465.
12 K.C. Chou, Biophys. J. 45 (1984) 881.
13 K.C. Chou, Biochem. J. 209 (1983) 573.
14 K.C. Chou, Biophys. J. 48 (1985) 289.
15 K.C. Chou, Biochem. J. 221 (1984) 27.
16 K.C. Chou, Biopolymers 26 (1987) 285.
17 K.C. Chou, Biophys. Chem., 30 (1988) 3.
18 E.B. Wilson, J.C. Decius and P.C. Cross, Molecular vibrations, (McGraw-Hill, New York, NY, 1955).
19 K. Itoh and T. Shimanouchi, Biopolymers 9 (1970) 383.
20 F.A. Cotton, Chemical application of group theory, 2nd edn., (Wiley-Interscience, New York, NY, 1971).